

國立交通大學

環境工程研究所

碩士論文

揮發性有機物在未飽和土壤中自然揮發之研究

**A Study on Natural Evaporation of VOC in Unsaturated
Soils**

研究生：俞仲豪

指導教授：葉弘德 教授

中華民國九十九年九月

揮發性有機物在未飽和土壤中自然揮發之研究

A Study on Natural Evaporation of VOC in Unsaturated Soils

研究生：俞仲豪

Student : Jung-Hau Yu

指導教授：葉弘德

Advisor : Hund-Der Yeh

國立交通大學

環境工程研究所



Submitted to Institute of Environmental Engineering

College of Engineering

National Chiao Tung University

in Partial Fulfillment of the Requirements

for the Degree of

Master of Science

in Environmental Engineering

September 2010

Hsinchu, Taiwan

中華民國九十九年九月

揮發性有機物在未飽和土壤中自然揮發之研究

研究生：俞仲豪

指導教授：葉弘德

國立交通大學環境工程研究所

摘要

地面儲存槽的洩漏，是土壤污染主要的污染源之一，發生滲漏後，部分揮發性有機物(volatile organic compound, VOC)會以非水相液體(NAPL)殘存在土壤中，若經過一段時間，氣相、液相、及吸附相的 VOC 會處於平衡狀態。若要整治受污染的土層，需先移除滲漏的儲存槽，隨後 VOC 將會在自然環境下逸散至大氣中，此自然揮發的過程，值得研究。VOC 存在土壤中，可分為純 VOC 和以多種化合物組成的複合 VOC 兩類，常見的汽油儲存槽滲漏污染問題，則以複合 VOC 污染居多。在本文中，我們發展了一個數值模式，描述複合 VOC 殘存相的揮發鋒面移動及地表下莫耳分率的空間分布，在模式中，考慮於揮發鋒面及其上下三個區域，透過有限差分法及可移動格網，近似求解莫耳分率的分佈。此外，考慮單一 VOC 污染的問題，將複合 VOC 模式簡化為單 VOC 模式，利用 Boltzmann' s transformation，求得單 VOC 模式的解析解。本文考慮六個污染案例，包括有無殘存相解之濃度分佈，以及不同土壤孔隙率、污染物、初始莫耳分率對揮發鋒面和莫耳分率分布之影響。藉由計算 VOC 揮發鋒面的位置和移動速度，本研究發展的模式，或可用來分析或評估受 VOC 污染的現地問題。

關鍵詞：解析解，數值模式，非水相液體，未飽和層，揮發鋒面

A Study on Natural Evaporation of VOC in Unsaturated Soils

Student : Jung-Hau Yu

Advisor : Hund-Der Yeh

Institute of Environmental Engineering

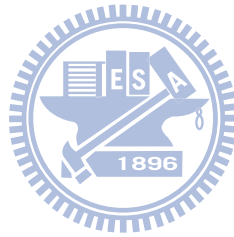
National Chiao Tung University

Abstract

Leak of underground storage tank is one of major sources for the spill of volatile organic compound (VOC) entering unsaturated soil. Once leak occurs, some VOCs may present in soil as residual non-aqueous phase liquid (NAPL) phase. The gas, liquid, and absorbed phases of VOC may reach equilibrium after a period of time in the soil. To clean up the contaminated soil, the tank must be removed and the VOC can then evaporate to the atmosphere. It is of interest to investigate the natural evaporation of NAPL. There are two types of VOC contamination in soil. One is multi-component VOC while the other is single-component VOC. Multi-component VOC, composed of several VOC components, is often found in petroleum leaking problems. This study develops a two-component model describing the mole fraction distributions of VOCs and migration of evaporation front of the VOC in NAPL phase in a homogeneous soil system. The model considers three regions which are above, below, and at the front and is solved by the finite difference method with a

moving grid approach. The model is also simplified to a single-component model which deals with a one-component VOC contamination and solved analytically by Boltzmann's transformation. Six cases are considered including a comparison of the solutions for the cases with and without the presence of residual NAPL phase and the assessment for the influences of different soil porosity, chemicals, and initial mole fraction on the front location and mole fraction. Finally, analytical expressions for the depth and moving speed of the front are also developed for practical uses.

Keywords: analytical solution, numerical model, NAPL, vadose zone, evaporation front.



誌謝

首先誠摯的感謝指導教授葉弘德，老師悉心的教導使我得以一窺地下水領域的深奧，不時的討論並指點我正確的方向，使我在這兩年中獲益匪淺。老師對學問的嚴謹更是我輩學習的典範。本論文的完成另外亦得感謝口試委員台灣大學吳先祺教授、逢甲大學馮秋霞教授、及本校葉立明教授，有你們的指正及建議，使得本論文能夠更完整而嚴謹。

感謝智澤、彥禎、士賓、博傑學長、雅琪、彥如、敏筠學姐、玳儀、其珊以及璟勝、庚轅、昭志、國豪、裕霖學弟們，這些日子，實驗室裏共同的生活點滴，學術上的討論，感謝眾位學長姐、同學、學弟的共同砥礪，你們的陪伴讓兩年的研究生活變得絢麗多彩，你們對於我的幫助我銘感在心。

最後，將本論文獻給我最摯愛的家人。

TABLE OF CONTENTS

摘要	I
ABSTRACT	II
致謝	IV
TABLE OF CONTENTS	V
LIST OF TABLES	VII
LIST OF FIGURES	VIII
NOTATION	X
CHAPTER 1 INTRODUCTION	1
1.1. Background	1
1.2. Literature Review	2
1.3. Objectives	4
CHAPTER 2 MATHEMATICAL MODEL	6
2.1 Mathematical model: Two-component case	6
2.1.1 Below the evaporation front	9
2.1.2 Above the evaporation front	10
2.1.3 At the evaporation front	11
2.1.4 Boundary and initial conditions	11
2.2 The numerical method in solving the model	13

2.2.1	Finite difference approximation -----	13
2.2.2	The solution procedure of the model -----	15
2.3	Simplified model: Single-component case -----	16
2.3.1	Below the evaporation front -----	16
2.3.2	Above the evaporation front -----	16
2.3.3	At the evaporation front -----	17
2.3.4	The analytical solution of single-component model -----	19
CHAPTER 3 RESULTS AND DISCUSSION -----		22
3.1	Case 1: Different evaporation times in two models -----	23
3.2	Case 2: Initial mole fraction -----	24
3.3	Case 3: Soil porosity -----	25
3.4	Case 4: Absence of the NAPL phase -----	26
3.5	Case 5: Different chemicals -----	27
3.6	Case 6: Effect of effective diffusion coefficient on moving speed of evaporation front-----	28
CHAPTER 4 CONCLUSIONS-----		29
REFERENCES-----		32

LIST OF TABLES

Tables	Page
1 Soil chemical properties used in case studies-----	36
2 Properties of carbon tetrachloride, toluene, and benzene-----	37



LIST OF FIGURES

Figures		Page
1	Schematic diagram of VOC contamination problem-----	38
2	Flowchart of the solution procedure for two-component model-----	39
3	Spatial distributions of mole fraction predicted by the single-component and two-component models at various evaporation times -----	40
4	The curves of the mole fraction versus depth at 100 day with various initial mole fractions-----	41
5	NAPL phase saturation versus mole fraction of benzene----	42
6	Normalized total concentration versus depth at 100 day for different values of soil porosity -----	43
7	The curves of normalized total concentration versus depth for single-component and simplified Jury et al.'s models at 100 day -----	44

8	Normalized total concentration versus time for single-component and simplified Jury et al.'s models at the depth of 1 m -----	45
9	Normalized total concentrations of carbon tetrachloride and toluene versus depth at 100 day -----	46
10	The curves of the depths of evaporation front versus evaporation time for carbon tetrachloride and toluene -----	47
11	Depth and Moving speed of evaporation front versus time for different effective diffusion coefficients -----	48



NOTATION

The following symbols are used in this thesis:

C_T = total concentration

C_L = liquid-phase concentration

C_S = adsorbed-phase concentration

C_G = gas-phase concentration

C_T^0 = saturated total concentration

C_L^0 = saturated liquid concentration

C_G^0 = saturated gas concentration

C_S^0 = saturated adsorbed concentration

C_G^P = equilibrium gas concentrations of pure component

C_L^P = equilibrium liquid concentrations of pure component

D_G^{air} = diffusion coefficient in air

D_G = diffusion coefficient in gas phase in soil

D_E = effective diffusion coefficient

f = mass fraction of organic compound in NAPL

i = number of component

u = mole fractions of organic compounds in the NAPL phase

u_0 = initial mole fraction

ϕ = soil porosity

s = evaporation front

θ_R = volumetric content of NAPL

θ_L = volumetric content of liquid-phase

θ_G = volumetric content of gas-phase

θ_R^0 = initial volumetric content of NAPL

θ_L^0 = initial volumetric content of liquid-phase

θ_G^0 = initial volumetric content of gas-phase

S_R = saturation of NAPL

S_L = saturation of liquid-phase

S_G = saturation of gas-phase

S_0 = initial NAPL saturation

t = time

z = depth from surface

ρ_R = density of NAPL

ρ_b = soil bulk density

K_H = Henry's Law constant

K_D = distribution coefficient

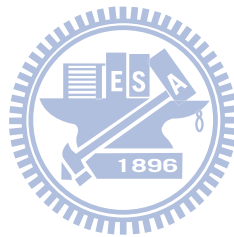
K_{oc} = organic carbon partition coefficient

f_{oc} = soil organic carbon fraction

P^0 = saturated vapor pressure of the VOC

M = molecular weight of the VOC

\mathfrak{R} = ideal gas constant



T = absolute temperature

L = depth of lower boundary

d = stagnant air boundary layer with thickness

dz = initial grid size

dz_r = grid size above the front

dz_{N-r} = grid size below the front

dt = time interval

U_f = moving speed of evaporation front

C = a constant parameter

η_i = $\phi S_G + (\phi S_w + \rho_b K_{Di}) / K_H$

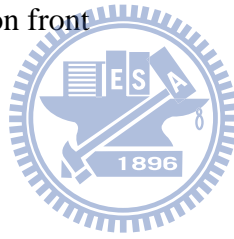
σ_i = $\rho_R \phi / C_{Gi}^P$

δ_i = η_i / D_G

μ_i = $\sigma_i M_i / D_G$

$F(u) = \delta_1 u + \mu_1 u [C - \delta_1 u - \delta_2 (1 - u)] / [\mu_1 u + \mu_2 (1 - u)]$

h = D_G^{air} / d



CHAPTER 1 INTRODUCTION

1.1 Background

Subsurface contamination by volatile organic compounds (VOCs) has been one of important issues to environmental problems recently. The pollution of VOCs is a common problem in nowadays, and VOCs may harm human health in skin and the respiratory system. The VOCs may enter subsurface soil from a variety of sources such as surface spill and leaking storage tank. They present in the unsaturated soil in different forms such as gas, liquid, adsorbed, and non-aqueous phase liquid (NAPL) phases. After a long residing time, the NAPL phase may be redistributed by water flow and turn into residual phase which is essentially held by surface tension and may stay in the soil pores over a long period of time.

The transport mechanisms of VOC in the unsaturated soil generally include advection, diffusion, dispersion, adsorption, volatilization, and chemical and biological reactions. Often diffusion is the dominating mechanism under natural condition, especially, for gas transport in a low-permeability soil. Advection is commonly ignored in studying organic vapor and gas migration in unsaturated soils (e.g., Jury et al., 1983; Zaidel and Russo, 1994; Yates et al., 2000). Falta et al. (1989) indicated that density driven advection is insignificant if the magnitude of soil permeability is less than $1 \times 10^{-11} \text{ m}^2$. Massmann and Farrier (1992) mentioned that the advection induced by atmospheric fluctuation is not substantial for gas transport in unsaturated soils with permeability less than $1 \times 10^{-14} \text{ m}^2$ under normal weather

conditions.

Soil vapor extraction (SVE) is an in-situ remedial technology for removing volatile constituents from unsaturated contaminated soils. In the cases of sparse VOC or low permeability formation, the removal efficiency of volatile compounds in soils will be significantly decreased. For this reason, diffusion may be the dominating mechanism for VOCs to move to a high permeability zone or volatilize to atmosphere under natural condition (Hoier et al., 2007). For nature evaporation, the upper boundary of the zone having NAPL phase becomes a front which moves downward with increasing time. The evaporation front of NAPL phase can therefore be defined as a moving boundary and the location of the moving boundary naturally represents the depth of NAPL. Moving boundaries are time-dependent and the position of the boundary has to be determined as a function of time and space (Crank, 1984). The moving boundaries occur mostly in heat-flow problems with phase changes and in some diffusion problems.

1.2 Literature Review

Jury et al. (1983) presented an analytical solution for a single pesticide species without NAPL phase undergoing first-order decay in an unsaturated zone. Sleep and Sykes (1989) presented a two-dimensional finite element model to simulate VOC partitioning to gas, liquid, solid and NAPL phases and its transport in unsaturated soils. They indicated that the partitioning rates between phases affected the VOC distribution significantly. Shoemaker et

al. (1990) used a method developed by Jury et al. (1983) to study the effect of vapor phase sorption on organic compounds transport. Their results showed that vapor phase sorption affects liquid phase organic concentration and also retards the rate of chemical migration toward the water table. Massmann and Farrier (1992) proposed a mathematical model to describe the transport of organic compounds in NAPL, gas, liquid, and adsorbed phases and used the finite difference approximation to simulate the movement of contaminants emanating from two point sources. Zaidel and Zazovsky (1999) developed a mathematical model to investigate the depletion of multi-component NAPL due to the evaporation and vapor transport in a SVE process. Yates et al. (2000) presented an analytical model to study the diffusion of organic vapors or other gases in layered soil systems.

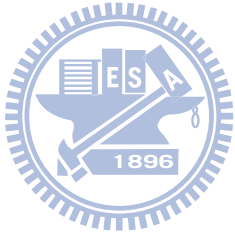


Moving boundary problems are also called Stefan problems referred to Stefan's investigations on the melting of the polar ice cap (Stefan, 1889a and b). Crank (1984) gave a literature survey on the Stefan problems occurring in physical and biological sciences, engineering, and decision and control theory, etc. Recently, studies involved moving boundaries were applied in the areas such as heat conduction [e.g., Cheng, 2000], solidification and melting processes [e.g., Feltham and Garside, 2001; Szimmat, 2002; Caldwell et al., 2003; Lee and Marchant, 2004; Rattanadecho, 2006; Naaktgeboren, 2007; Patnaik et al., 2009], dissolution [e.g., Quintard and Whitaker, 1995; Vazquez-Nava and Lawrence, 2009], and evaporation [e.g., Purlis and Salvadori, 2009; Sazhin et al., 2010].

1.3 Objectives

The purpose of this thesis is to develop a two-component model to predict the mole fraction distributions of VOC and the migration of evaporation front of NAPL phase after the removal of the storage tank in a homogeneous unsaturated soil. To the best of our knowledge, the existing models in simulating the natural evaporation of VOC in unsaturated soil have the problem domains all with fixed boundaries. In contrast, the present model considers a moving boundary to describe the downward move of evaporation front of NAPL phase. The front, which migrates downward with time, is treated as a lower boundary while the land surface is used as the upper boundary for the region above the front. For the region below the front, the front becomes the upper boundary and the lower boundary is located at some distance below the land surface. Based on the present model with these boundaries, VOC mole fraction distributions and the front location are solved by the finite difference method with a moving grid approach. This numerical model can predict the mole fraction distributions between two components and the movement of the front, analyze evaporation time of VOC, and assess the influences of initial mole fraction, soil porosity as well as chemical volatility on VOC migration in the unsaturated soil. Moreover, a single-component model is obtained from simplifying the two-component model and solved analytically using Boltzmann's transformation. Then, an analytical expression for the moving speed of the front can be developed from the solution and used to assess the time of

vanish of NAPL at a specific location below the land surface.



CHAPTER 2 METHMETICL MODEL

This chapter presents the mathematical models and related solution procedures for VOC transport in homogeneous and unsaturated soils.

2.1. Mathematical model: Two-component case

Figure 1(a) shows a leaking storage tank located on the top of land surface and filled with VOC. Consider that the VOC leaking from the tank has four different phases (namely, gas, liquid, adsorbed and residual NAPL phases) and distributes uniformly in the unsaturated zone. Each phase has a saturated or equilibrium concentration and constant volumetric content. The VOC has an initial NAPL saturation S_0 in the soil. The saturation of each phase denotes as the volume percentage in the soil pore and the sum of saturation of each phase equals one. The evaporation front of the NAPL, denoted as $s(t)$, initially stays right at the land surface, i.e., $z = s(t) = 0$ where z is the vertical axis, and moves downward with increasing time. Figure 1(b) shows the contamination scenario in which the gas phase VOC begins to evaporate to atmosphere and the NAPL starts to vaporize to gas phase after the tank being removed. Assume that the NAPL phase of VOC evaporates fully above the front and the front migrates instantaneously when the evaporation occurs. In other words, the VOC presents only in gas, liquid, and adsorbed phases and the NAPL saturation, S_R , equals zero between the land surface and the front. Below the front, the residual VOC still exists. At the front, volatilization occurs from NAPL phase to gas phase instantaneously and the content

of NAPL transferring to gas phase follows the conservation of mass.

The total concentration of VOC is the sum of the concentration of each phase; that is:

$$C_T = C_G\theta_G + C_L\theta_L + C_S\rho_b + \rho_R\theta_R \quad (1)$$

where C_G , C_L , and C_S represent the chemical concentrations in the gas, liquid, and adsorbed phases, respectively, and ρ_b and ρ_R are the soil bulk density and density of NAPL, respectively. The symbols θ_G , θ_L , and θ_R are the volumetric contents of gas, liquid, and NAPL phases, respectively, and denote as

$$\theta_G = \phi S_G, \quad \theta_L = \phi S_L, \quad \text{and} \quad \theta_R = \phi S_R \quad (2)$$

where ϕ is the soil porosity and S_G and S_L are gas and liquid saturations, respectively.

The equilibrium relationships between the gas and liquid phases as well as the liquid and adsorbed phases may be expressed, respectively, as

$$C_G = K_H C_L \quad \text{and} \quad C_S = K_D C_L = K_{oc} f_{oc} C_L \quad (3)$$

where K_H is Henry's Law constant, K_D is the distribution coefficient, K_{oc} is the organic carbon partition coefficient, and f_{oc} is the soil organic carbon fraction. The equilibrium relationships given in Equation (3) are linear and reversible and their coefficients are dependent on different chemical characteristics and soil properties.

The equation of mass conservation for those four phases in the unsaturated soil is (Corapcioglu and Baehr, 1987)

$$\frac{\partial}{\partial t} [C_G \theta_G + C_L \theta_L + C_S \rho_b + \rho_R \theta_R] + \nabla J_G = 0 \quad (4)$$

where $J_G = -D_G \nabla C_G$ is the vapor flux and D_G is the soil-gas diffusion coefficient. A tortuosity factor accounting for the reduced flow area and increased path length of diffusing molecules in soil can be related to the soil porosity and the fluid content in the soil.

Millington and Quirk (1961) defined that

$$D_G = D_G^{air} \left(\frac{\theta_G^3}{\phi^2} \right) \quad (5)$$

where D_G^{air} is the air-gas diffusion coefficient.

Consider that VOC has multiple components. Substituting Equations (2) and (3) into Equation (4), the mass-conservation equation in three dimension for those four phases in the unsaturated soil becomes (Zaidel and Zazovsky, 1999)

$$\frac{\partial [nS_G C_{Gi} + (nS_L + \rho_b K_{Di}) C_{Li}] + \rho_R \phi \frac{\partial (S_R f_i)}{\partial t}}{\partial t} = \nabla \cdot (D_G \nabla C_{Gi}) \quad (6)$$

with

$$C_{Gi} = C_{Gi}^p \frac{f_i / M_i}{\sum f_j / M_j}, \quad C_{Li} = C_{Li}^p \frac{f_i / M_i}{\sum f_j / M_j} \quad (7)$$

$$\sum_{i=1}^{N_c} f_i = 1 \quad (8)$$

where C_G^p and C_L^p are equilibrium gas and liquid concentrations of pure component, respectively, f is the mass fraction of organic compound in NAPL, i is the number of each component, and N_C is the total number of organic compounds. The saturated gas phase

concentration for pure component can be estimated from the idea gas law as

$$C_G^P = P^0 M / \mathfrak{R} T \quad (9)$$

where P^0 is the saturated vapor pressure of the VOC, M is the molecular weight of the VOC, \mathfrak{R} is the ideal gas constant, and T is the absolute temperature.

To describe the behavior of volatilization of VOC from NAPL phase to gas phase, the evaporation front is introduced as a moving boundary in the unsaturated soil. The problem domain for VOC transport with a moving boundary in the soil can be divided into three regions. The VOC transport equations in these three regions are described below.

2.1.1 Below the evaporation front



In this region, NAPL phase exists and the saturation of NAPL phase is greater than zero, i.e., $S_R > 0$. Equation (8) can then be expressed as

$$\sum_{i=1}^{N_c} u_i = 1 \quad (10)$$

with u_i representing mole fractions of organic compounds in the NAPL phase, i.e.,

$u_i = C_{Gi} / C_{Gi}^P$. For a one-dimensional system, Equation (6) becomes:

$$\eta_i \frac{\partial u_i}{\partial t} + \sigma_i \frac{\partial (S_R u_i M_i / \sum u_j M_j)}{\partial t} = D_G \frac{\partial^2 u_i}{\partial z^2} \quad (11)$$

where $\eta_i = \phi S_G + (\phi S_W + \rho_b K_{Di}) / K_H$ and $\sigma_i = \rho_R \phi / C_{Gi}^P$. For a two-component VOC and

based on Equation (11), the mass-conservation equation for each component can be written

as:

$$\eta_1 \frac{\partial u_1}{\partial t} + \sigma_1 \frac{\partial(S_R M_1 u_1 / M_1 u_1 + M_2 u_2)}{\partial t} = D_G \frac{\partial^2 u_1}{\partial z^2} \quad (12)$$

$$\eta_2 \frac{\partial u_2}{\partial t} + \sigma_2 \frac{\partial(S_R M_2 u_2 / M_1 u_1 + M_2 u_2)}{\partial t} = D_G \frac{\partial^2 u_2}{\partial z^2} \quad (13)$$

Select $u = u_1$ as a primary variable. The saturation of NAPL phase can be obtained from

Equation (12) as

$$S_R = \frac{[C - \delta_1 u - \delta_2(1-u)][M_1 u + M_2(1-u)]}{\mu_1 u + \mu_2(1-u)} \quad (14)$$

where $\delta_i = \eta_i / D_G$, $\mu_i = \sigma_i M_i / D_G$, and C is a constant parameter computed by the initial

NAPL saturation S_0 and mole fraction u_0 of component one as:

$$C = \delta_1 u^0 + \delta_2(1-u^0) + S_0 \frac{\mu_1 u^0 + \mu_2(1-u^0)}{M_1 u^0 + M_2(1-u^0)} \quad (15)$$

Substituting Equations (10) and (14) into Equation (12) yields

$$\frac{\partial F(u)}{\partial t} = \frac{\partial^2 u}{\partial z^2} \quad (16)$$

where $F(u) = \delta_1 u + \mu_1 u [C - \delta_1 u - \delta_2(1-u)] / [\mu_1 u + \mu_2(1-u)]$.

2.1.2 Above the evaporation front

In this region the NAPL phase fully evaporates. i.e., $S_R = 0$. For a two-component

VOC, Equation (11) can be written for each component as follows:

$$\delta_1 \frac{\partial u_1}{\partial t} = \frac{\partial^2 u_1}{\partial z^2} \quad (17)$$

$$\delta_2 \frac{\partial u_2}{\partial t} = \frac{\partial^2 u_2}{\partial z^2} \quad (18)$$

where u_1 and u_2 represent normalized concentrations above the evaporation front,

2.1.3 At the evaporation front

Assume that the evaporation of NAPL phases occurs instantaneously and the sum of mole fraction equals one, i.e., $u_1+u_2 = 1$. Combining Equations (12) and (13), the equation for mass conservation at the front can be expressed as

$$\frac{\partial S_R}{\partial t} = \left(\frac{D_G}{\sigma_1} \right) \frac{\partial^2 u_1}{\partial z^2} + \left(\frac{D_G}{\sigma_2} \right) \frac{\partial^2 u_2}{\partial z^2} - \left(\frac{\eta_1}{\sigma_1} \right) \frac{\partial u_1}{\partial t} - \left(\frac{\eta_2}{\sigma_2} \right) \frac{\partial u_2}{\partial t} \quad (19)$$

Taking the limits of $\Delta t \rightarrow 0$ and $\Delta z \rightarrow 0$, Equation (18) describing the front can then be written as

$$\lim_{\Delta t \rightarrow 0} \frac{0 - S_R + \frac{\eta_1}{\sigma_1} (u_1^{t+} - u_1^{t-}) + \frac{\eta_2}{\sigma_2} (u_2^{t+} - u_2^{t-})}{\Delta t} = \lim_{\Delta z \rightarrow 0} \frac{D_G}{\sigma_1} \left(\frac{\partial u_1^{z+}}{\partial z} - \frac{\partial u_1^{z-}}{\partial z} \right) + \frac{D_G}{\sigma_2} \left(\frac{\partial u_2^{z+}}{\partial z} - \frac{\partial u_2^{z-}}{\partial z} \right)}{\Delta s} \quad (20)$$

where the superscripts $t+$ and $t-$ of the mole fraction in Equation (20) denote the mole fraction at the time slightly after and before the volatilization, respectively, and $z+$ and $z-$ represent the mole fraction at the region slightly below and above the front, respectively. Equation (20)

can be further simplified as

$$\frac{ds}{dt} = \frac{\frac{D_G}{\sigma_1} \left(\frac{\partial u_1^{z+}}{\partial z} - \frac{\partial u_1^{z-}}{\partial z} \right) + \frac{D_G}{\sigma_2} \left(\frac{\partial u_2^{z+}}{\partial z} - \frac{\partial u_2^{z-}}{\partial z} \right)}{\frac{\eta_1}{\sigma_1} (u_1^{t+} - u_1^{t-}) + \frac{\eta_2}{\sigma_2} (u_2^{t+} - u_2^{t-}) - S_R} \quad (21)$$

2.1.4 Boundary and initial conditions

For simulating the ambient environment near the surface, the gas phase VOC is

considered to diffuse across a stagnant air boundary layer with thickness d and the gas phase concentration is assumed equal to zero at the top of boundary layer. The flux diffusing to the atmosphere can then be expressed as (Jury et al., 1983)

$$D_G \frac{\partial C_G}{\partial z} = h \frac{C_T}{R_G}, \text{ at } z = 0 \quad (22)$$

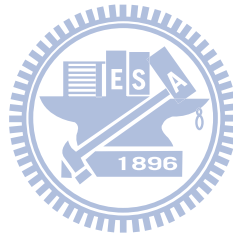
where $h = D_G^{air} / d$. If the thickness of air boundary layer near the surface is very small and negligible, one may assume that $d = 0$. Equation (22) can then be expressed as

$$C_T = 0, \text{ at } z = 0 \quad (23)$$

For a multicomponent VOC, the upper boundary conditions can be written from Equation (23)

as

$$u_1(0, t) = u_2(0, t) = 0 \quad (24)$$



The conditions of the mole fractions at the lower boundary are denoted as:

$$u_1(L, t) = u^o, \quad u_2(L, t) = 1 - u^o \quad (25)$$

where L is the depth of the lower boundary.

The initial NAPL saturation and the mole fractions of each component are assumed spatially uniform; they are

$$S_R(z, 0) = S_0 \quad (26)$$

$$u_1(z, 0) = u^o, \quad u_2(z, 0) = 1 - u^o \quad (27)$$

The evaporation front is initially located at the land surface and thus denoted as

$$s(0) = 0 \quad (28)$$

2.2 The numerical method in solving the model

This section presents the numerical method used to solve the two-component model.

2.2.1 Finite difference approximation

The equations of describing VOC transport in the three regions are solved separately by the finite difference method. An interpolative moving grid approach (Javierre et al. 2006) is adopted to handle the moving boundary problem. The total number of nodes within the problem domain is equal to N and r is the nodal number assigned at the evaporation front beginning from the land surface. Accordingly, the number of grids from the land surface to the front is $r-1$, the number of grids below the front is $N-r$, and the initial grid size dz is equal to $L/(N-1)$. The grid sizes above and below the front defined as dz_r and dz_{N-r} , respectively, need to be re-estimated after each move of the front. To avoid introducing large truncation error, the grid sizes dz_r and dz_{N-r} should be close to dz . If the front move to a location between the nodal numbers initially assigned as j and $j+1$, the new grid sizes of dz_r and dz_{N-r} are then estimated by $s/(r-1)$ and $(L-s)/(N-r)$, respectively, where $r = j+1$. The backward difference relative to time and central difference relative to space are used to approximate the VOC transport equations. Therefore, the difference equation for the mole fraction in the

region below the front obtained from Equation (16) is

$$\frac{F(u_j^n) - F(u_j^{n-1})}{dt} = \frac{u_{j+1}^n - 2u_j^n + u_{j-1}^n}{(dz_{N-r})^2}, \quad s(t) < z \leq \infty \quad (29)$$

where n is the number of time step, and dt is the time interval. The difference equations for

the mole fractions of the two components in the region above the front obtained from

Equations (17) and (18) are, respectively:

$$\delta_1 \frac{u_{1j}^n - u_{1j}^{n-1}}{dt} = \frac{u_{1(j+1)}^n - 2u_{1j}^n + u_{1(j-1)}^n}{(dz_r)^2}, \quad 0 \leq z < s(t) \quad (30)$$

$$\delta_2 \frac{u_{2j}^n - u_{2j}^{n-1}}{dt} = \frac{u_{2(j+1)}^n - 2u_{2j}^n + u_{2(j-1)}^n}{(dz_r)^2}, \quad 0 \leq z < s(t) \quad (31)$$

Finally, the difference equations for the mole fractions of the two components at the front also derived from Equations (17) and (18) with different grid sizes above and below the

front are, respectively, expressed as

$$\left(\frac{\delta_1}{2}\right) \frac{u_{1r}^n - u_{1r}^{n-1}}{dt} = \frac{dz_r u_{1(r+1)}^n + dz_{N-r} u_{1(r-1)}^n - (dz_r + dz_{N-r}) u_{1r}^n}{(dz_r + dz_{N-r}) dz_r dz_{N-r}}, \quad z = s(t) \quad (32)$$

$$\left(\frac{\delta_2}{2}\right) \frac{u_{2r}^n - u_{2r}^{n-1}}{dt} = \frac{dz_r u_{2(r+1)}^n + dz_{N-r} u_{2(r-1)}^n - (dz_r + dz_{N-r}) u_{2r}^n}{(dz_r + dz_{N-r}) dz_r dz_{N-r}}, \quad z = s(t) \quad (33)$$

Substituting Equation (10) into Equation (21), the difference equation for the front location

can then be obtained as

$$\frac{s^n - s^{n-1}}{dt} = \frac{\frac{D_G}{\sigma_1} \left(\frac{u_{1(r+1)}^n - u_{1r}^n}{dz_{N-r}} - \frac{u_{1r}^n - u_{1(r-1)}^n}{dz_r} \right) + \frac{D_G}{\sigma_2} \left(\frac{u_{1r}^n - u_{1(r+1)}^n}{dz_{N-r}} - \frac{1 - u_{1r}^n - u_{2(r-1)}^n}{dz_r} \right)}{\frac{\eta_1}{\sigma_1} (u_{1r}^n - u_{1r}^{n-1}) + \frac{\eta_2}{\sigma_2} (u_{1r}^{n-1} - u_{1r}^n) - S_R} \quad (34)$$

2.2.2 The solution procedure of the model

Because the location of the evaporation front $s(t)$ is unknown, a trial and error procedure is therefore taken to find the front location. The steps of the procedure are listed below and the related flowchart is shown in Figure 2:

1. Give the initial front location (Equation (28)) and nodal values of mole fraction based on the boundary conditions (Equations (24) and (25)) and initial conditions (Equations (26) and (27)).
2. Guess front location after the start of evaporation.
3. Determine the nodal number for the front and the grid sizes based on the front location.
4. Solve the solutions for the region below the front (Equation (29)), for the region above the front (Equations (30) and (31)), and at the front (Equations (32) and (33)).
5. Compute the front location based on Equation (34).
6. Proceed to next time step if the location of the front converges, i.e., the difference between two succeeding estimations of the front location is less than a very small value, e.g., 10^{-10} m; otherwise, go back to step 3.



2.3 Simplified model: Single-component case

This section presents a single-component model with the governing equation simplified from the two-component model. The domain of the single-component model is also divided into three regions based on the front location. In a one-dimensional homogeneous and unsaturated soil system, Equation (6) representing the VOC transport can be written as

$$\frac{\partial C_T}{\partial t} - D_G \frac{\partial^2 C_G}{\partial z^2} = 0 \quad (35)$$

2.3.1 Below the evaporation front

In this region, the NAPL has not vaporized to gas phase yet. The VOC concentrations in each phase are the initial saturated concentrations and the total concentration can be expressed as

$$C_T = C_T^0 = C_G^P \theta_G^0 + C_L^P \theta_L^0 + C_S^P \rho_b + \rho_R \theta_R^0 \quad (36)$$

where C_S^P is the saturated VOC concentrations for pure component in adsorbed phases, C_T^0 is the initial total concentration, and θ_G^0 , θ_L^0 , and θ_R^0 are the initial volumetric contents, respectively.

2.3.2 Above the evaporation front

In this region, NAPL phase of the VOC completely vaporizes to gas phase; therefore, the VOC presents only in gas, liquid, and adsorbed phases, i.e., $C_T = C_G \theta_G + C_L \theta_L + C_S \rho_b$. Jury et al. (1983) used a ratio R to represent each phase in relation to the total concentration.

Accordingly, one may introduce the following equation based on Equations (1) and (3):

$$C_T = R_G C_G = R_L C_L = R_S C_S \quad (37)$$

where the ratios are $R_G = \theta_G + \theta_L/K_H + \rho_b K_D/K_H$, $R_L = \theta_G K_H + \theta_L + \rho_b K_D$, and

$$R_S = \theta_G K_H / K_D + \theta_L / K_D + \rho_b.$$

With Equation (37), Equation (35) can be written as

$$\frac{\partial C_T}{\partial t} - D_E \frac{\partial^2 C_T}{\partial z^2} = 0 \quad (38)$$

where $D_E = D_G / R_G$ denotes as effective diffusion coefficient. Equation (38) describes the

VOC transport in gas and liquid phases between the land surface and evaporation front. In

reality, the volatilization of NAPL occurs right at the evaporation front which will be discussed in the next section.



2.3.3 At the evaporation front

The evaporation front moves downward while the NAPL vaporizes to the gas phase.

Assume that the transformation of the contents between these two phases occurs

instantaneously and the liquid volumetric content is unchanged, i.e., $\theta_L = \theta_L^0$. In addition,

the VOC concentrations in each phase are still saturated, i.e., $C_G = C_G^P$, $C_L = C_L^P$, and $C_S =$

C_S^P . The total concentration at the front can therefore be expressed as

$$C_T = C_T^0 \quad (39)$$

The gas, liquid, and NAPL phases remain in the unsaturated soil pores, the sum of θ_G , θ_L , and

θ_R equals soil porosity ϕ , i.e., $\theta_G + \theta_L + \theta_R = \phi$. Assumes ϕ does not change with time, the transformation of volumetric content with respect to time among each phase is conserved.

Thus,

$$\frac{\partial \theta_G}{\partial t} + \frac{\partial \theta_L}{\partial t} = -\frac{\partial \theta_R}{\partial t} \quad (40)$$

Since $\partial \theta_L / \partial t = 0$, one can get $\partial \theta_G / \partial t = -\partial \theta_R / \partial t$ from Equation (40). In addition, the bulk density ρ_b does not change with time, i.e., $\partial \rho_b / \partial t = 0$. Therefore, one can obtain the following relationship from Equation (1)

$$\frac{\partial C_T}{\partial t} = (\rho_R - C_G^P) \frac{\partial \theta_R}{\partial t} \quad (41)$$

With Equation (41) and taking the limits of $\Delta t \rightarrow 0$ and $\Delta z \rightarrow 0$, Equation (35) describing the front can then be written as

$$\lim_{\Delta t \rightarrow 0} (\rho_R - C_G^P) \frac{\theta_R^+ - \theta_R^-}{\Delta t} = \lim_{\Delta z \rightarrow 0} \frac{D_E \left(\frac{\partial C_T^+}{\partial z} - \frac{\partial C_T^-}{\partial z} \right)}{\Delta z} \quad (42)$$

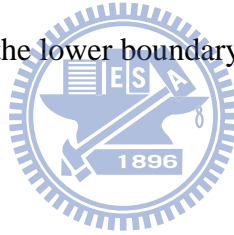
where the superscripts + and - denote the volumetric content at the time slightly after and before the volatilization, respectively, and the concentrations at the region slightly below and above the front, respectively. Consider that the volatilization occurs instantaneously, therefore θ_R^+ equals θ_R^0 and θ_R^- equals zero after evaporation. The VOC concentrations in each phase are the initial saturated concentrations below the front and the concentration gradient of gas phase below the front is naturally equal to zero, i.e., $\partial C_G^+ / \partial z = 0$. Since the liquid density is higher than the gas phase concentration about three

orders (Falta et al., 1989, Tables 1 and 4), the term related to C_G^P on the left-hand side of Equation (42) is thus negligible. Accordingly, Equation (43) representing the front $z = s(t)$ can be expressed as

$$\theta_R^0 \rho_R \frac{ds}{dt} = D_E \frac{\partial C_T^-}{\partial z} \quad (43)$$

2.3.4 The analytical solution of single-component model

Consider that the VOC is saturated or in equilibrium state in different phases and uniformly distributed in the unsaturated soil initially. The mathematical model describing the single-component VOC transport in the soil consists of Equation (38) as the governing equation, Equations (39) and (43) as the lower boundary conditions, and Equation (23) as the upper boundary condition.



Based on Boltzmann's transformation, a new variable is defined as $\xi = z / 2\sqrt{D_E t}$.

Equation (38) can then be transformed to an ordinary differential equation as

$$\frac{d^2 C_T}{d\xi^2} + 2\xi \frac{dC_T}{d\xi} = 0 \quad (44)$$

The solution of Equation (44) can be obtained as (Carslaw and Jaeger, 1959)

$$C_T(\xi) = A \cdot \text{erf}(\xi) + B \quad (45)$$

where $\text{erf}(\xi)$ is the error function and A and B are unknown coefficients. Substituting

Equation (45) into Equation (23), the result for the concentration distribution is

$$C_T(z, t) = A \times \operatorname{erf}\left(\frac{z}{2\sqrt{D_E t}}\right) \quad (46)$$

Substituting Equation (39) into Equation (46), the evaporation front $s(t)$ and coefficient A can then be obtained, respectively, as

$$s(t) = \alpha\sqrt{t} \quad (47)$$

$$A = \frac{C_T^0}{\operatorname{erf}\left(\frac{\alpha}{2\sqrt{D_E}}\right)} \quad (48)$$

where α is an unknown constant depending upon the soil parameters and contaminant characteristics.



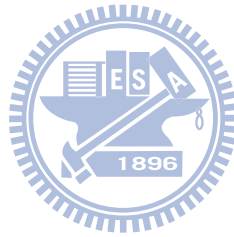
The time of vanish of NAPL can be solved by Newton's method (Yeh, 1987) from Equation (47) when the front reaches a target location below the land surface designated by the environmental or legal requirement. In addition, the moving speed of the evaporation front can also be obtained after taking the derivative of Equation (47) with respect to time and the result is

$$U_f = \frac{\alpha}{2\sqrt{t}} \quad (49)$$

Substituting Equations (46), (47) and (48) into Equation (43) yields

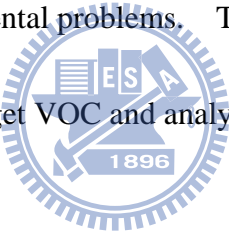
$$\frac{\theta_R^0 \rho_R \alpha}{2} = \frac{D_E C_T^0 \exp\left(-\frac{\alpha^2}{4D_E}\right)}{\sqrt{\pi D_E} \operatorname{erf}\left(\frac{\alpha}{2\sqrt{D_E}}\right)} \quad (50)$$

The unknown constant α can then be easily determined from Equation (50) by Newton's method. Note that the normalized total concentration is defined as $C_T(z,t)/C_T^0$, representing the mole fraction in the single-component model.



CHAPTER 3 RESULTS AND DISCUSSION

Leaks of petroleum fuels from the underground storage tanks are common problems for soil contamination. The petroleum spills are often associated with aromatic hydrocarbons such as benzene, toluene, ethyl benzene, and various xylene isomers (BTEX). In this section, the hydrocarbons of benzene and toluene are chosen to simulate their transport and mole fraction distributions in unsaturated soils using the two-component model. In the past, Carbon tetrachloride was commonly used as coolant in industry or produced as the fire extinguishers. Carbon tetrachloride is highly toxic; a small amount of this chemical residing in the soil may pose severe environmental problems. The carbon tetrachloride in the unsaturated soil is considered as a target VOC and analyzed using the single-component model.



Six cases are considered to address the issues in regard to the evaporation rate, evaporation front movement, mole fraction, and concentration distributions of VOC for the present models. Case 1 is to compare the mole fractions of toluene at various evaporation times predicted by single-component and two-component models. Case 2 examines the effect of initial mole fraction on the evaporation and the changes of the mole fraction distributions of benzene and toluene. Case 3 investigates the effect of soil porosity on vaporization of carbon tetrachloride from NAPL phase to gas phase while case 4 addresses the issue of carbon tetrachloride transport based on the model with and without considering

the presence of NAPL phase. Case 5 studies the migrations of evaporation front for different contaminants, namely carbon tetrachloride and toluene. Case 6 discusses the effect of effective diffusion coefficient of carbon tetrachloride on the moving speed of evaporation front. The values of the soil chemical properties are listed in Table 1 and the properties of benzene, toluene, and carbon tetrachloride are given in Table 2 for these six cases. Note that the depth of the lower boundary L is chosen as 5 m, the total number of nodes N is 10000, and the time interval dt is 0.1 sec in the case study when adopting the finite different approximation for the two-component model.

3.1 Case 1: Different evaporation times in two models

This case uses the same assumptions for both single-component and two-component models and considers that toluene is the only VOC found in the soil, i.e., $u_0 = 1$. Figure 3 shows the mole fraction distributions of toluene versus depth predicted by the single-component and two-component models at various evaporation times. The dashed line denotes the solution of single-component model while the solid line represents the results predicted by the two-component model. Moreover, the symbols of rhombus, triangle, and circle represent the mole fractions at times 1, 10, and 100 day, respectively. This figure shows the front locations at various evaporation times and at the front the mole fraction equals its initial value for the single-component VOC. The figure also shows that the curves predicted by both models are fairly close, implying that the results predicted by the

two-component model with the present numerical approach match well with those estimated based on the analytical solution of the single-component model. The moving speeds of the front U_f estimated by equation (49) are 8.296×10^{-2} , 2.624×10^{-2} , and 8.296×10^{-3} m/day at times 1, 10, and 100 day, respectively, indicating that the moving speed decreases rapidly at early time and then slowly as time increases

3.2 Case 2: Initial mole fraction

In this case, benzene is considered to be component one and toluene is component two in the two-component model. Figures 4(a) - 4(c) show the mole fraction distributions of benzene and toluene versus depth when the initial mole fractions of component one are 0.2, 0.5, and 0.8, respectively, at 100 day. The evaporation front of the NAPL with $u_0 = 0.2, 0.5,$ and 0.8 reaches 0.860, 0.931, and 1.002 m below the surface, respectively. In addition, at the front $u_1 = 0.123$ and $u_2 = 0.877$ when $u_0 = 0.2$, $u_1 = 0.310$ and $u_2 = 0.690$ when $u_0 = 0.5$, and $u_1 = 0.498$ and $u_2 = 0.502$ when $u_0 = 0.8$. The figures show that the depth of the front increases with the initial mole fraction of benzene, representing the moving speed of the front depends on the initial mole fraction. The mole fraction of benzene increases with depth until reaching $u_1 = u_0$; on the other hand, the mole fraction of toluene increases above the front but decreases below the front until reaching $u_2 = 1 - u_0$. These results indicate that at the front, the mole fraction of benzene decreases as time increases while that of toluene increases with time. Moreover, the mole fractions of both components are not equal to their initial values at

the front. In fact, both components reach their initial values occurred at certain distances below the front. Such a phenomenon can be attributed to the fact that benzene has higher evaporation efficiency than toluene. Therefore, the mole fractions of benzene and toluene change with depth, although the NAPL below the front does not evaporate. Figure 5 shows the curve of NAPL phase saturation, calculated from Equation (14), versus mole fraction of benzene. The figure demonstrates that S_R equals 0.004 when $u_0 = 0$ and 0.015 when $u_0 = 1$. This result indicates that S_R changes with mole fraction and varies slightly below the front.

3.3 Case 3: Soil porosity

This case examines the effect of soil porosity on the concentration distribution of carbon tetrachloride using the single-component model. The total evaporation time is considered to be 100 day. Note that the saturation S of each phase is constant and the volumetric contents θ of gas, liquid, and NAPL change in equal proportion with the soil porosity. Figure 6 shows the predicted normalized total concentration versus depth at 100 day for the porosities of 0.1, 0.3, and 0.5. It is apparent from Figure 4 that the vaporization increases moderately with soil porosity. In addition, the evaporation front of the NAPL with $\phi = 0.1, 0.3,$ and 0.5 are at 0.831, 1.432, and 1.860 m below the land surface, respectively, and the moving speeds of the front are 4.154×10^{-3} , 7.158×10^{-3} , and 9.301×10^{-3} m/day, respectively, indicating that the moving speed of the front increases with soil porosity although different amounts of NAPL exist in the soil.

3.4 Case 4: Absence of the NAPL phase

In this case, the effects of presence and absence of NAPL on the distribution of carbon tetrachloride in the soil are compared and studied. Jury et al. (1983) considered the scenario that there were three phases of VOC presented in the soil with neglecting the NAPL phase. Their analytical model included the mechanisms of diffusion, soil water advection, and first-order decay. They used a diffusive flux as the upper boundary condition at the land surface and zero total concentration at infinite depth as the lower boundary condition. Jury et al.'s model is simplified by neglecting the water phase advection and decay and thus called simplified Jury et al.'s model hereafter.




Figure 7 shows the curves of normalized total concentration of carbon tetrachloride versus depth predicted by two different VOC transport models at $t = 100$ day. The solid line with triangle symbol represents the normalized total concentration distribution predicted by the present single-component model while the solid line with circle predicted by simplified Jury et al.'s model. Figure 7 indicates that the normalized total concentration of VOC predicted by the present model is significantly higher than that of simplified Jury et al.'s model. Although NAPL occupies only one-percent of volume in the soil pores, the NAPL however affects the total concentration distribution and transport capability greatly. Figure 8 exhibits the predicted distribution of normalized total concentration versus time for the present model and simplified Jury et al.'s model at the depth of 1 m. The figure shows that

the total concentration of carbon tetrachloride decreases quickly after 2 day predicted by simplified Jury et al.'s model and after 37 day by the single-component model indicating that the presence of NAPL has significant impact on the VOC transport.

3.5 Case 5: Different chemicals

In this case, both carbon tetrachloride and toluene are considered to reside in the unsaturated soil. Table 2 shows that toluene has less molecular weight and liquid density and lower saturated vapor pressure and Henry's law constant than those of carbon tetrachloride. Figure 9 shows the curves of normalized total concentration versus depth for carbon tetrachloride and toluene at 100 day predicted by the single-component model for each chemical. The solid lines with circle and triangle represent the concentration distributions of carbon tetrachloride and toluene, respectively. The vaporization of toluene is significantly lower than that of carbon tetrachloride; the depths of the evaporation front of carbon tetrachloride and toluene equal 1.659 m and 0.813 m, respectively, at 100 day. Figure 10 shows that the depths of the front versus evaporation time for both chemicals. This figure indicates that the fronts at 50 day and 100 day reach the depths of 1.173 m and 1.659 m, respectively, for carbon tetrachloride and 0.575 m and 0.813 m, respectively, for toluene. Obviously, the migration of the front of carbon tetrachloride is significantly faster than that of toluene due to lower vapor pressure and Henry's Law constant value of toluene. Such a phenomenon results in lower vapor pressure gradient and proportion of concentration in gas

and liquid phases. In addition, the diffusion coefficients of gas and liquid phases of both chemicals differ by four orders of magnitude. Thus the diffusion of liquid phase is significantly lower than that of gas phase.

3.6 Case 6: Effect of effective diffusion coefficient on moving speed of evaporation front

Equation (49) shows the moving speed of evaporation front U_f which in fact represents the evaporation rate of NAPL in soil. This case investigates the effect of the soil chemical properties on U_f based on the single-component model. The D_E is a function of soil porosity, volumetric content of each phase, air diffusion coefficient, soil bulk density, Henry's Law constant, and organic carbon fraction. Obviously, different soil chemical properties will affect the value of D_E . Figure 11 shows the curves of the depth and moving speed of the front versus evaporation time for $D_E = 10^{-10}$, 10^{-9} , 10^{-8} , and 10^{-7} m²/s. The depth of the front increases with time and D_E greatly while the moving speed is maximal when VOC begins to evaporate and then decreases with increasing time for a fixed value of D_E .

CHAPTER 4 CONCLUSIONS

This thesis presents a two-component model to describe the mole fraction distributions of VOC in the unsaturated soil. In the model, zero-concentration is chosen as the upper boundary condition and a moving boundary representing the evaporation front of NAPL is the lower boundary in the region where the NAPL evaporates fully. In the region below the front, the NAPL phase prevails. The upper boundary of this region is the evaporation front and the lower boundary is relatively far away from the front and thus chosen at infinity. The model is solved by the finite difference method with a moving grid approach. This numerical model is applied to predict the mole fraction distributions between two components and the movement of the front in the soil. In addition, the numerical model is also used to analyze evaporation time of VOC and assess the influences of initial mole fraction, soil porosity as well as chemical volatility on VOC migration. The two-component model is further simplified to a single-component model, which is solved analytically based on Boltzmann's transformation. In addition, analytical expressions are also developed for the front and its moving speed as functions of evaporation time, characteristics of soil and VOC, and volumetric content of each phase.

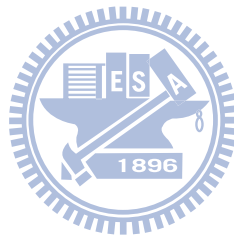
Both two-component and single-component models have been used to study the problems of the evaporation rate, evaporation front movement, mole fraction, and concentration distributions of VOC through six designed cases. Based on the results of these case studies,

following conclusions can be drawn:

1. The VOCs such as benzene and toluene usually have different transport efficiencies. The predicted results from the two-component model indicate that the initial mole fraction of each component has affects on the location of evaporation front and the mole fraction distributions. As the result, the depth of the front increases with the initial mole fraction for benzene but decreases with that for toluene.
2. The NAPL distributions after evaporation for single-component and two-component VOCs are different. For the single-component case, the total VOC concentration at or below the front is always equal to the initial concentration; however, for two-component case the mole fractions of VOC at the front will change with time base on different evaporation efficiencies of two components. In other words, both the mole fractions and NAPL phase saturation change with depth below the front for a two-component VOC.
3. The migration distance of the evaporation front of NAPL increases with evaporation time and soil porosity. As a result, the NAPL phase will vaporize to gas phase and vanishes slowly with increasing time.
4. The normalized total concentration of VOC in the case without the presence of NAPL will be significantly lower than that with the presence of the NAPL. Even if the volumetric content of NAPL is extremely small, it still affects the transport efficiency greatly.

5. Gas phase diffusion is the dominating transport mechanism for VOC migration in the unsaturated soil. Since Toluene has lower values of vapor pressure and Henry's Law constant than those of carbon tetrachloride, the migration of the evaporation front of toluene is therefore significantly slower than that of carbon tetrachloride.

6. Both the depth and moving speed of evaporation front increase with the effective diffusion coefficient. Moreover, the depth of the front increases with time while the moving speed of the front decreases with increasing time.



References

- Baehr, A. L., 1987. Selective transport of hydrocarbons in the unsaturated zone due to aqueous and vapor phase partitioning. *Water Resour. Res.* 23 (10), 1926-1938.
- Caldwell, J., Kwan, Y.Y., 2003. On the perturbation method for the Stefan problem with time-dependent boundary conditions. *Int. J. Heat Mass Transfer.* 46, 1497–1501.
- Cheng, T.F., 2000. Numerical analysis of nonlinear multiphase Stefan problem. *Comput. Struct.* 75, 225-233.
- Carslaw, H. S., Jaeger, J. C., 1959. Conduction of heat in solids. 2nd ed., Clarendon, Oxford,
- Corapcioglu, M.Y., Baehr, A.L., 1987. A compositional multiphase model for groundwater contamination by petroleum products. *Water Resour. Res.* 23(1), 191-200.
- Crank, J., 1984. Free and moving boundary problems. *Oxford Univ. Press, New York,*
- Falta, R. W., Javandel, I., Pruess, K., Witherspoon, P. A., 1989. Density-driven flow of gas in unsaturated zone due to evaporation of the volatile organic compounds. *Water Resour. Res.* 25(10), 2159-2169.
- Feltham, D.L., Garside, J., 2001. Analytical and numerical solutions describing the inward solidification of a binary melt. *Chem. Eng. Sci.* 56, 2357-2370.
- Fetter, C.W., 1993. Contaminant hydrogeology. *Prentice Hall, New Jersey.*
- Hoier, C. K., Sonnenborg, T. O., Jensen, K. H., Kortegaard, C., Nasser, M. M., 2007.

Experimental investigation of pneumatic soil vapor extraction. *J. Cont. Hydrol.* 89, 29-47.

Javierre, E., Vuik, F.J., Vermolen, S., Zwaag, van der, 2006. A comparison of numerical models for one-dimensional Stefan problems. *J. Comput. Appl. Math.* 192, 445-459.

Jury, W. A., Spencer, W. F., Farmer, W. J., 1983. Behavior assessment model for trace organics in soil: I. Model description. *J. Environ. Qual.* 12 (4), 558-564.

Jury, W., A., Russo, D., Streile, G., EL Abd H., 1990. Evaluation of volatilization by organic chemicals residing below the soil surface. *Water Resour. Res.* 26 (1), 13-20.

Lee, M.Z.C., Marchant, T.R., 2004. Microwave thawing of cylinders. *Appl. Math. Modell.* 28, 711-733.



Massmann, J., Farrier, D., 1992. Effects of atmospheric pressure on gas-transport in the vadose zone. *Water Resour. Res.* 28(3), 777-791.

Millington, R. J., Quirk, J. M., 1961. Permeability of porous solids. *Trans. Faraday Soc.* 57, 1200-1207.

Naaktgeboren, C., 2007. The zero-phase Stefan problem. *Int. J. Heat Mass Transfer.* 50, 4614-4622.

Patnaik, S., Voller, V.R., Parker, G., Frascati, A., 2009. Morphology of a melt front under a condition of spatial varying latent heat. *Int. Comm. Heat Mass Transfer.* 36, 535-538.

Perry, R. H., Green, D.W., Maloney, J.Q., 1997. Perry's chemical engineers' handbook. 7th ed., McGraw-Hill, New York.

Pinder, G. F., Abriola, L. M., 1986. On the simulation of nonaqueous phase organic compounds in the subsurface. *Water Resour. Res.* 22 (9), 109S-119S.

Purlis, E., Salvadori, V.O., 2009. Bread baking as a moving boundary problem. Part 1: Mathematical modelling. *J. Food Eng.* 91, 428–433.

Purlis, E., Salvadori, V.O., 2009. Bread baking as a moving boundary problem. Part 2: Model validation and numerical simulation. *J. Food Eng.* 91, 434–442.

Quintard, M., Whitaker, S., 1995. The mass flux boundary condition at a moving fluid-fluid interface. *Ind. Eng. Chem. Res.* 34, 3508–3513.

Rattanadecho, S., 2006. Simulation of melting of ice in a porous media under multiple constant temperature heat sources using a combined transfinite interpolation and PDE methods. *Chem. Eng. Sci.* 61, 4571–4581.

Sazhin, S.S., Krutitskii, P.A., Gusev, I.G., Heikal, M.R., 2010. Transient heating of an evaporating droplet. *Int. J. Heat Mass Transfer.* 53, 2826–2836.

Shoemaker, C. A., Culver, T. B., Lion, L. W., Peterson, M. G., 1990. Analytical models of the impact of two-phase sorption on subsurface transport of volatile chemicals. *Water Resour. Res.* 26 (4), 745-758.

- Sleep, B. E., Sykes, J. F., 1989. Modeling the transport of volatile organics in variably saturated media. *Water Resour. Res.* 25 (1), 81-92.
- Stefan, J., 1889. Sber. Akad. Wiss. Wien. 98, 473-484.
- Stefan, J., 1889. Sber. Akad. Wiss. Wien. 98, 965-983.
- Szimmat, J., 2002. Numerical simulation of solidification processes in enclosures. *Heat and Mass Transfer.* 38, 279-293.
- Vazquez-Nava, E., Lawrence, C., Thermal dissolution of a spherical particle with a moving boundary. *Heat Transfer Eng.* 30(5), 416-426.
- Yates, S. R., Papieri, S. K., Gao, F., Gan, J., 2000. Analytical solutions for the transport of volatile organic chemicals in unsaturated layered systems. *Water Resour. Res.* 36(8), 1993-2000.
- Yeh, H. D., 1987. Theis' solution by nonlinear least-squares and finite- difference Newton's method, *Ground Water.* 25(6), 710-715.
- Zaidel, J., Russo, D., 1994. Diffusive transport of organic vapors in the unsaturated zone with kinetically-controlled volatilization and dissolution: analytical model and analysis. *J. of Contam. Hydro.* 17, 145-165.
- Zaidal, J., Zazovsky, A., 1999. Theoretical study of multicomponent soil vapor extraction: propagation of evaporation-condensation fronts. *J. of Contam. Hydro.* 37, 225-268.

Table 1

Soil chemical properties used in case studies

Property	Symbol	Value
Soil porosity	ϕ	0.4
Initial NAPL saturation	S_R^0	0.01
Initial liquid saturation	S_L^0	0.3
Initial gas saturation	S_G^0	0.69
Air diffusion coefficient (m ² /s) ^a	D_G^{air}	5×10^{-6}
Water diffusion coefficient (m ² /s) ^a	D_L^{water}	5×10^{-10}
Temperature (°C)	T	20
Soil organic carbon fraction	f_{oc}	0.0125
Soil bulk density (g/m ³) ^a	ρ_b	1.59×10^6
Depth of the lower boundary (m)	L	5

^a Cited from Jury et al. (1983)

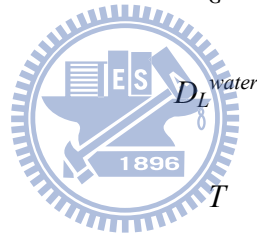


Table 2

Properties of carbon tetrachloride, toluene, and benzene (Perry et al., 1997)

		Carbon tetrachloride	Toluene	Benzene
Property	Symbol		Value	
Molecular weight (g/mole)	M	153.8	92.1	78.1
NAPL density (g/m ³)	ρ_R	1.584×10^6	8.62×10^5	8.79×10^5
Saturated vapor pressure (kPa)	P	12.13	2.9	10.3
Henry's law constant	K_H	0.958	0.26	0.22
Organic carbon partition coefficient (m ³ /g)	K_{oc}	1.1×10^{-4}	1.4×10^{-4}	8.3×10^{-5}



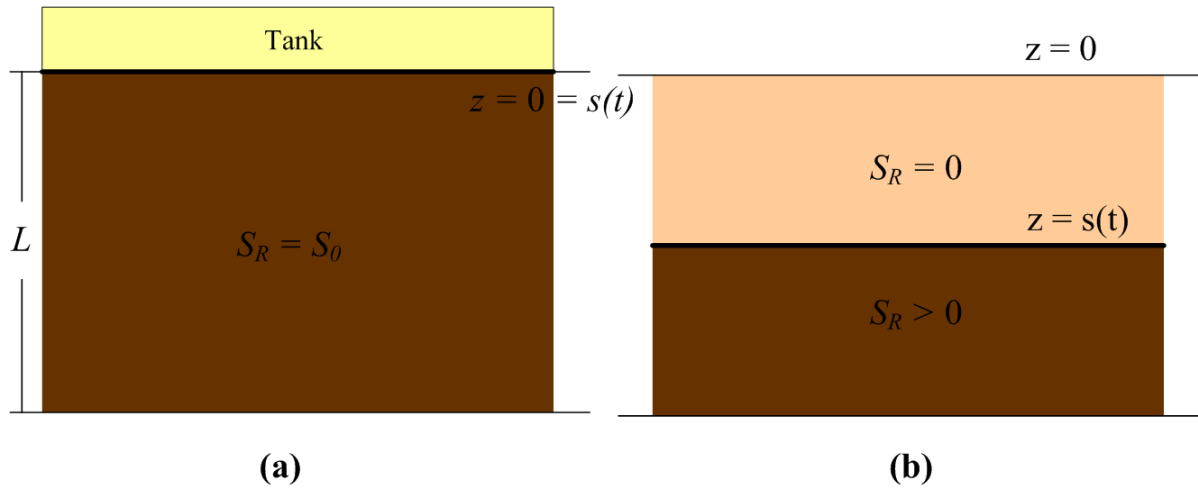
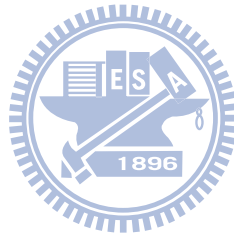


Figure 1. Schematic diagram of VOC contamination problem, where (a) VOC reaches equilibrium between each phase, and (b) VOC begins to evaporate after the tank is removed.



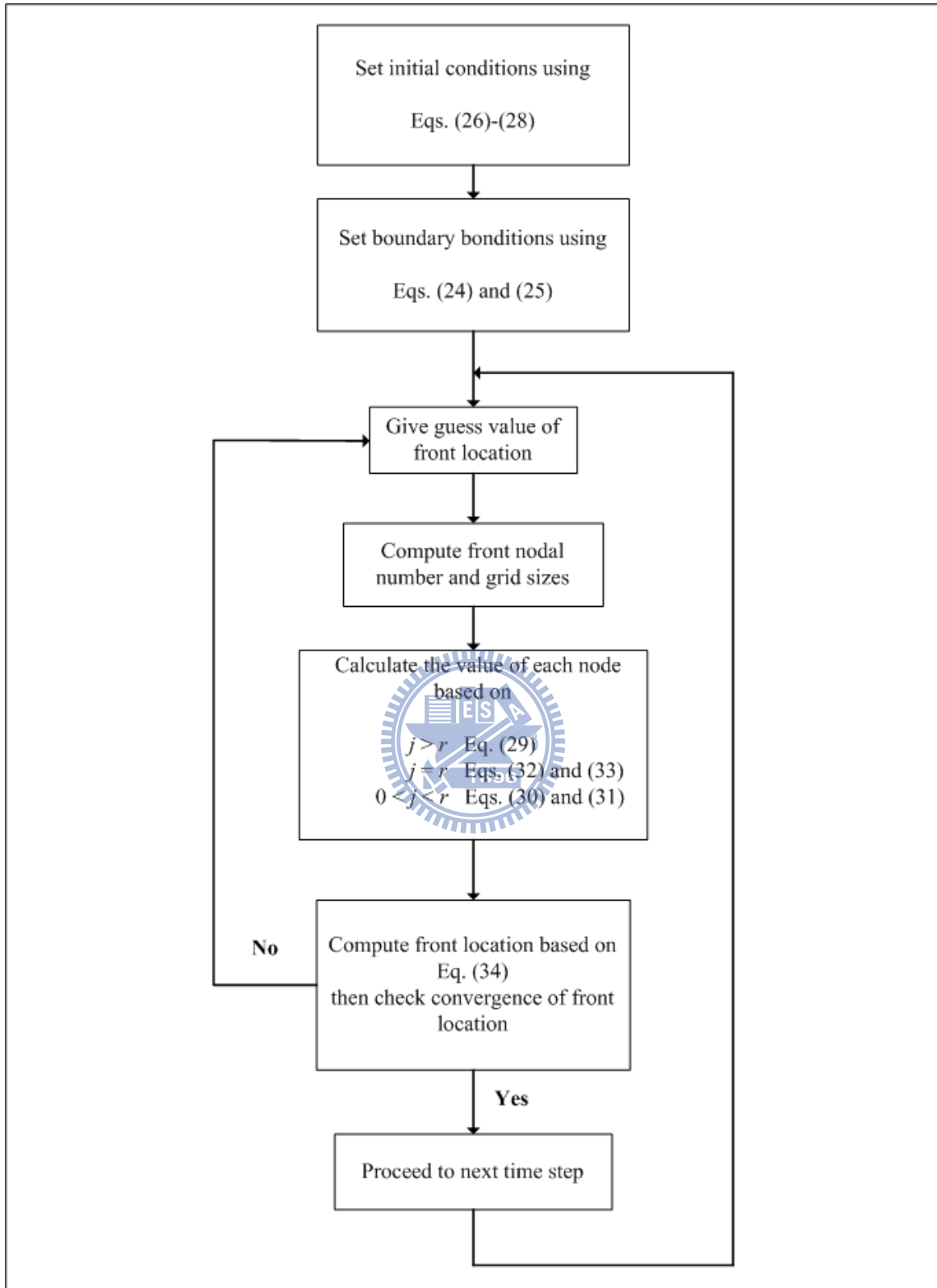


Figure 2. Flowchart of the solution procedure for the two-component model.

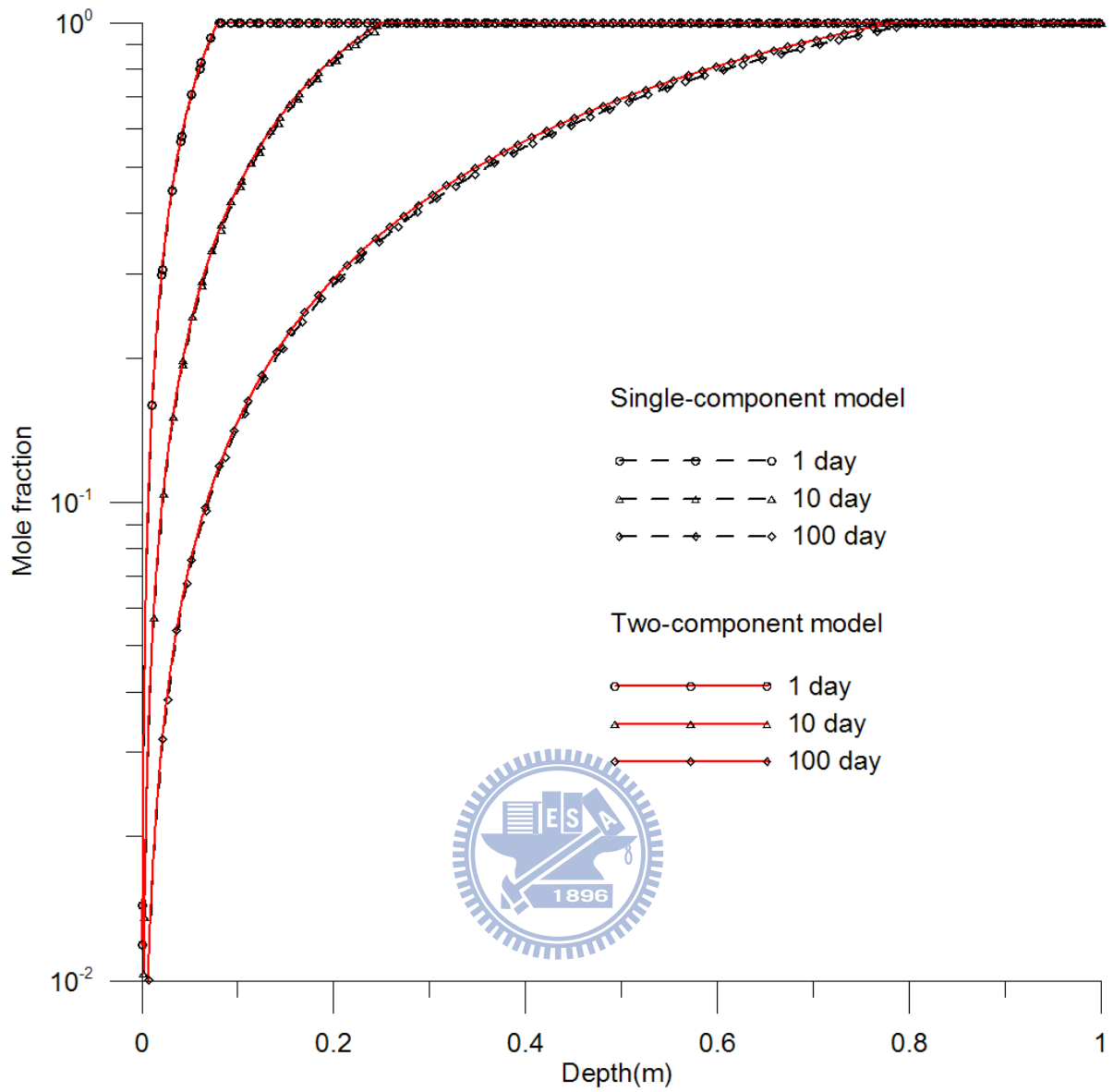


Figure 3. Spatial distributions of mole fraction predicted by the single-component and two-component models at various evaporation times.

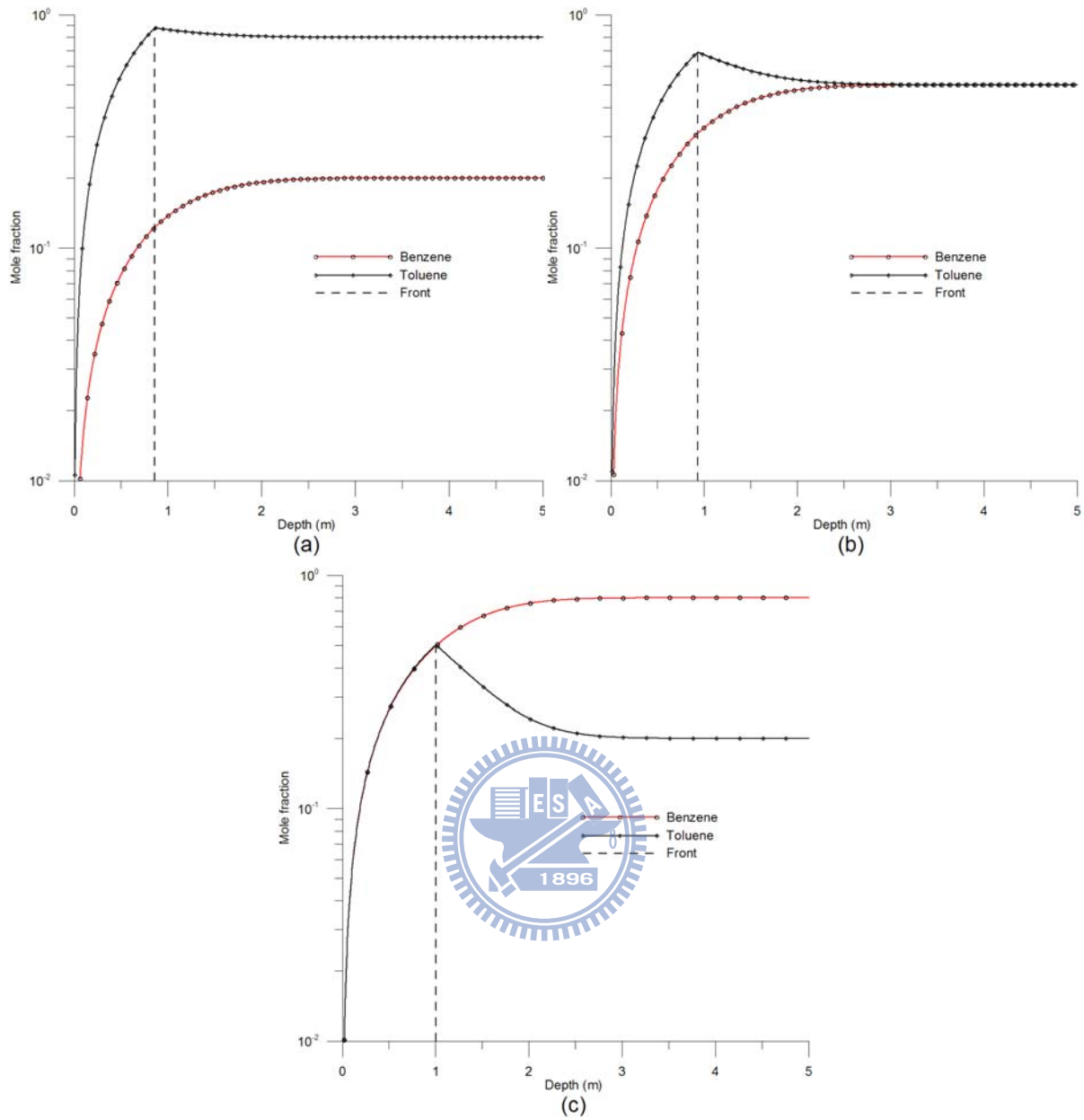


Figure 4. The curves of the mole fraction versus depth at 100 day when the initial mole fraction of benzene equals (a) 0.2, (b) 0.5, and (c) 0.8.

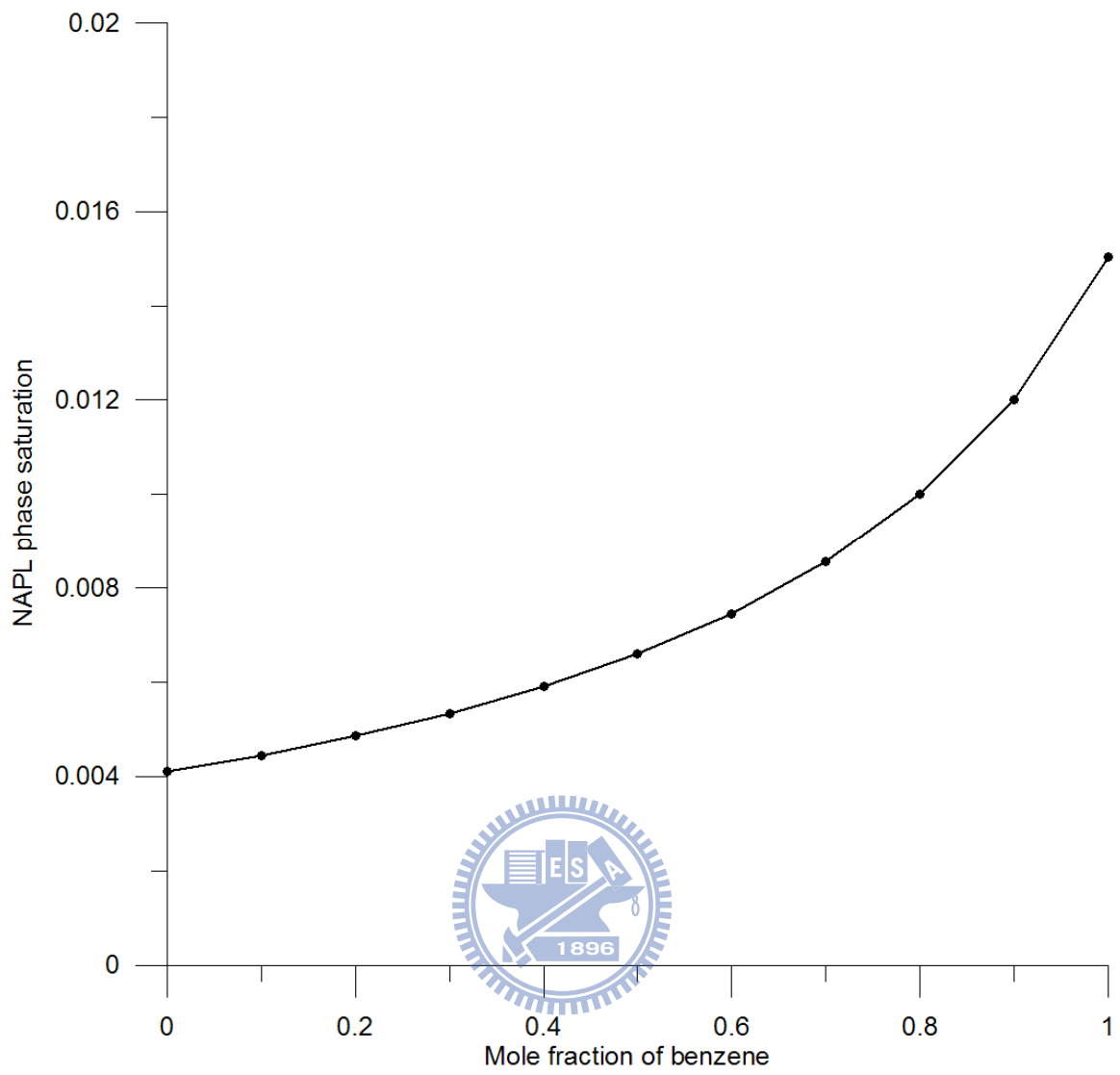


Figure 5. NAPL phase saturation versus mole fraction of benzene.

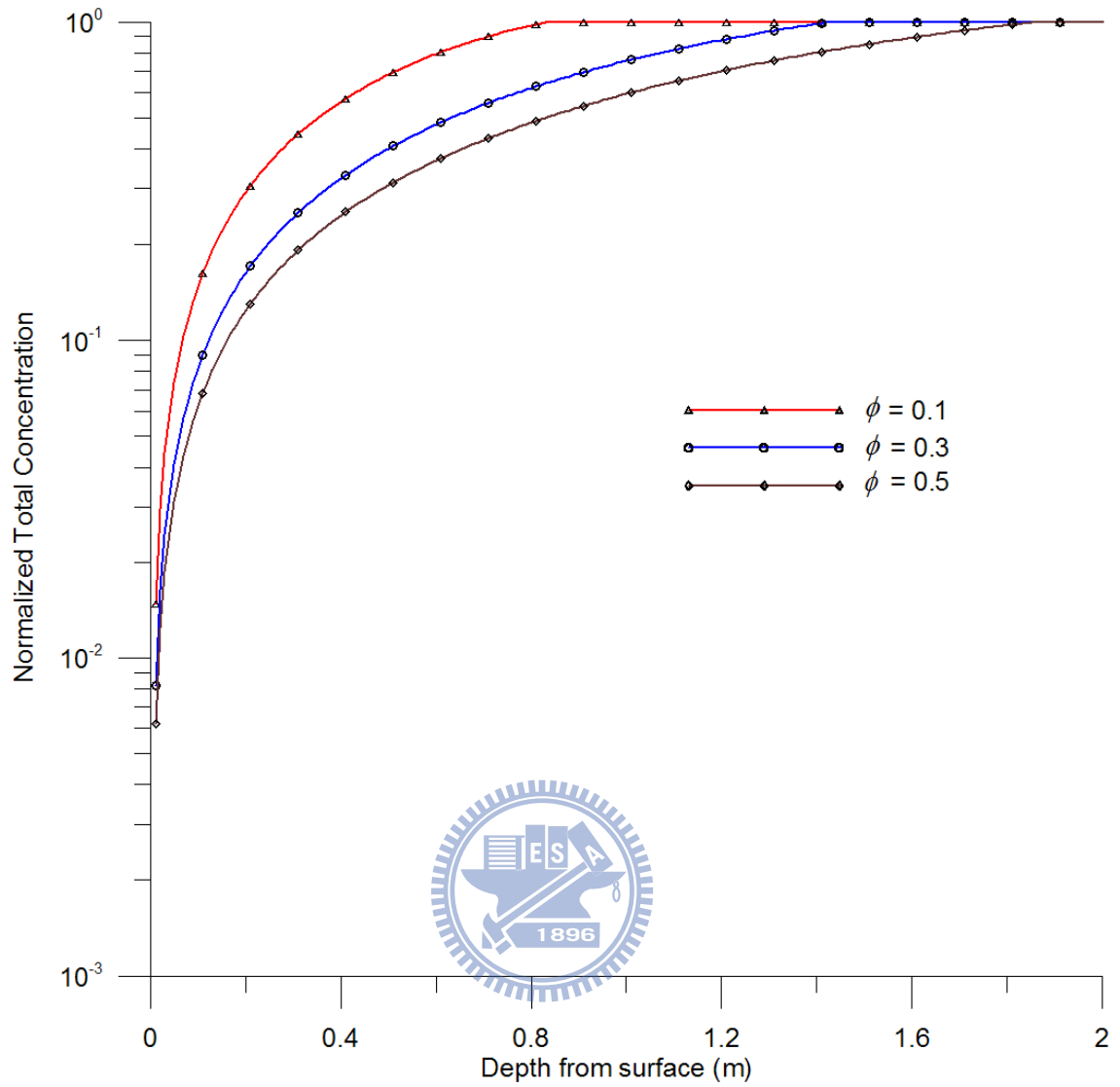


Figure 6. Normalized total concentration versus depth at 100 day for different values of soil porosity.

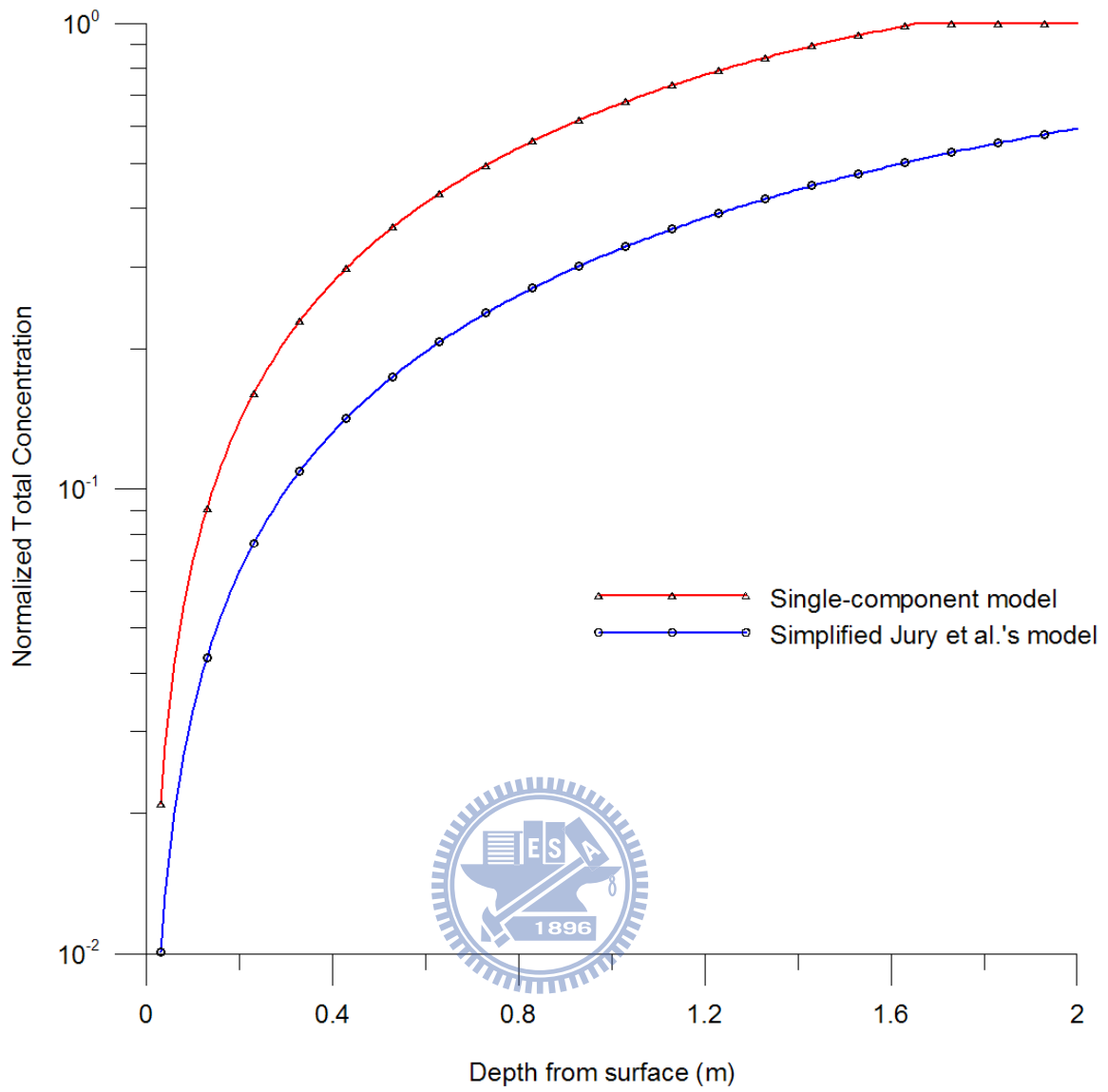


Figure 7. The curves of normalized total concentration versus depth for single-component and simplified Jury et al.'s models at 100 day.

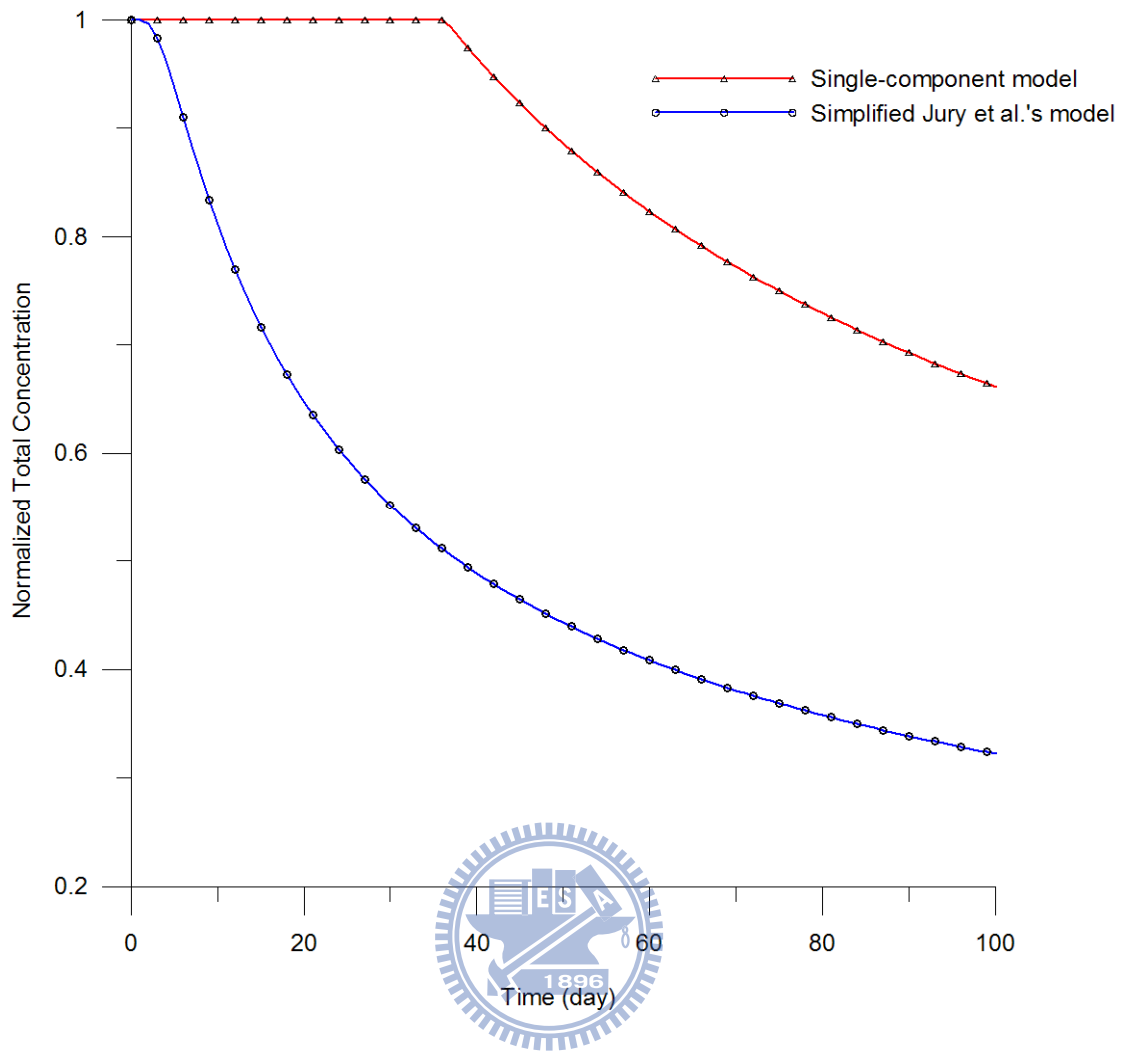


Figure 8. Normalized total concentration versus time for single-component and simplified Jury et al.'s models at the depth of 1 m .

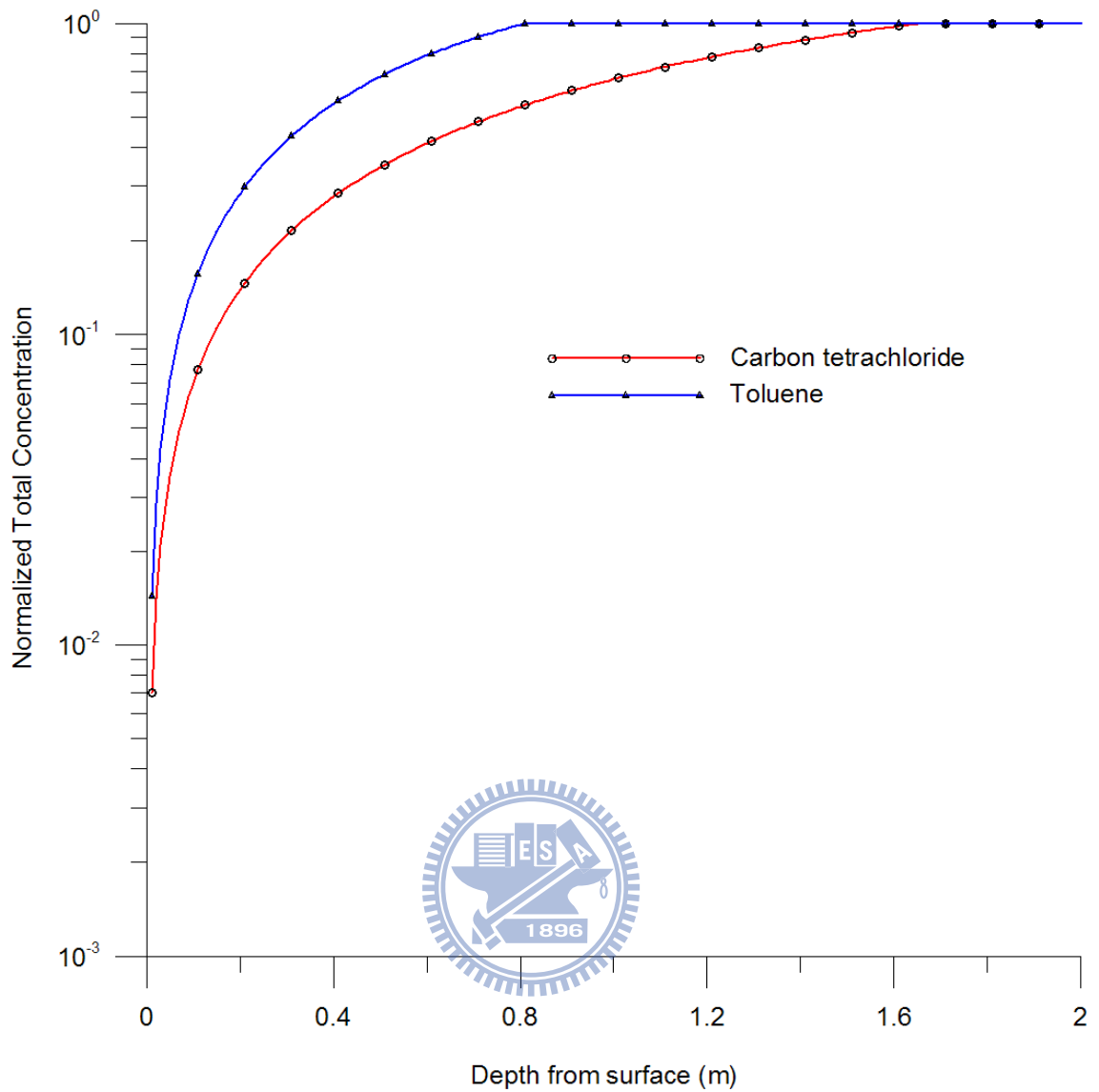


Figure 9. Normalized total concentrations of carbon tetrachloride and toluene versus depth at 100 day.

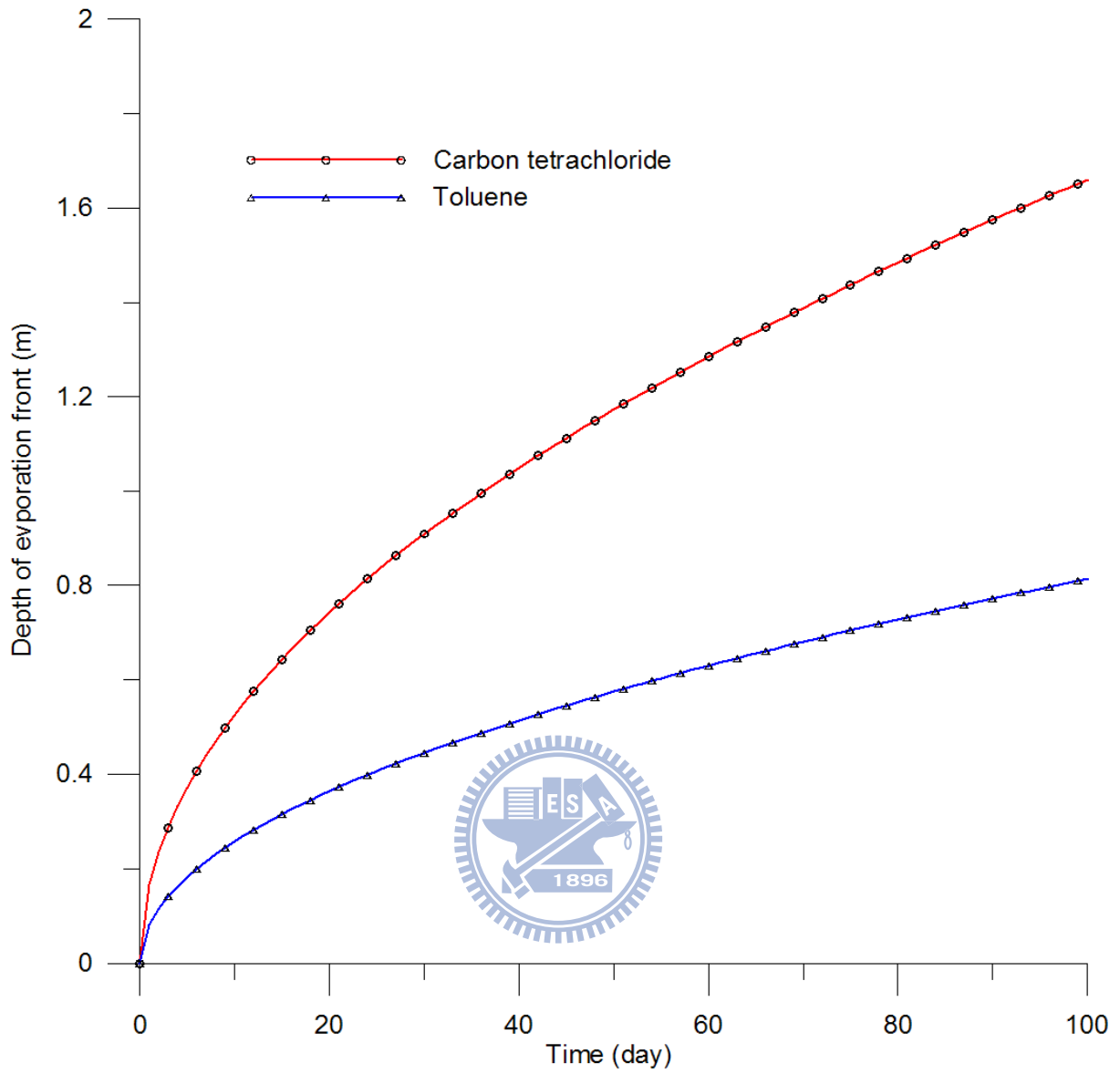


Figure 10. The curves of the depths of evaporation front versus evaporation time for carbon tetrachloride and toluene.

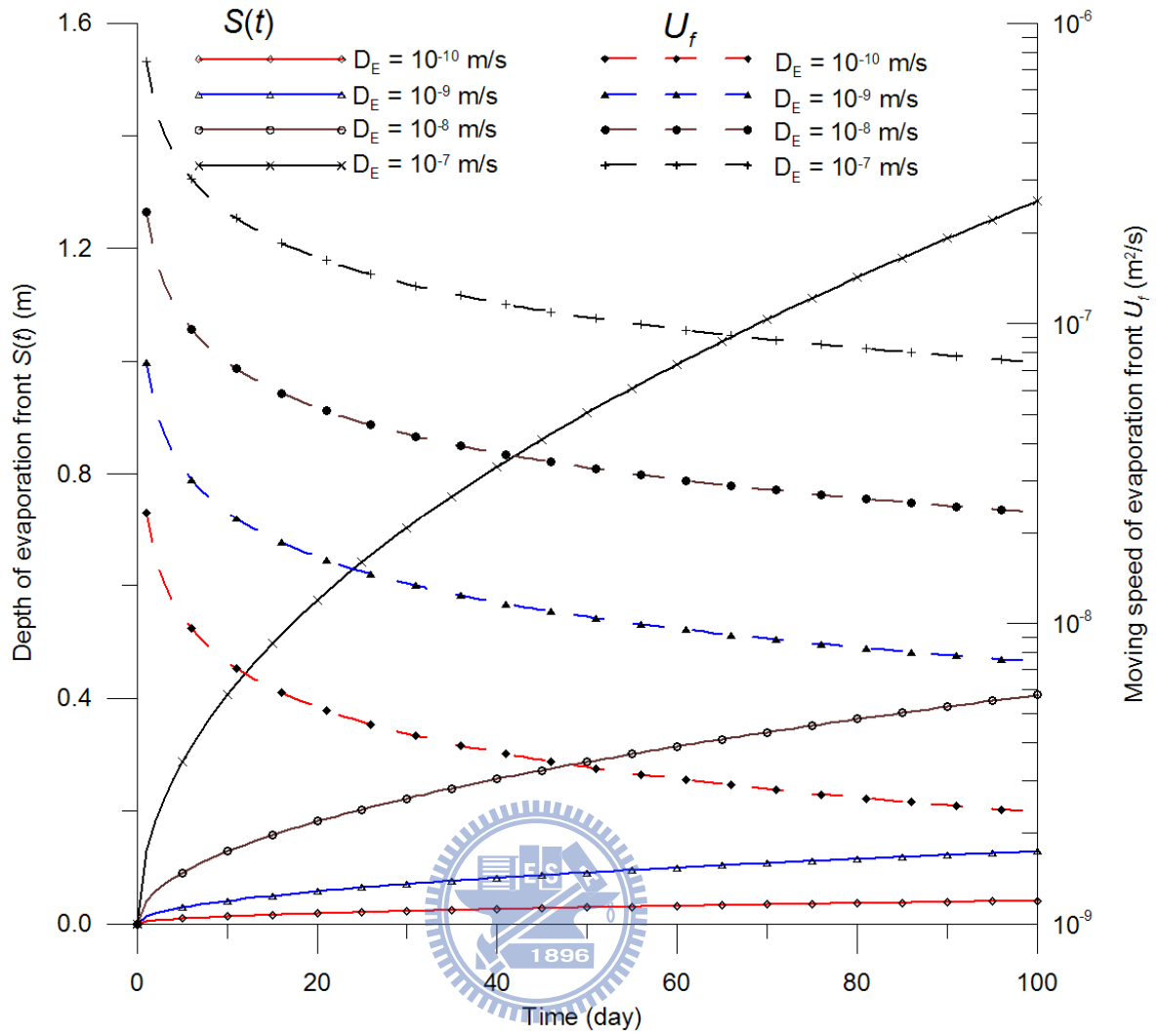


Figure 11. Depth and Moving speed of evaporation front versus time for different effective diffusion coefficients.